water

MDPI

Article

Novel Cosmic Ray Neutron Sensor Accurately Captures Field-Scale Soil Moisture Trends under Heterogeneous Soil Textures

Kade D. Flynn [1,†], Briana M. Wyatt [2,*] and Kevin J. McInnes [2]

[1] Department of Soil, Water, and Climate, University of Minnesota, St. Paul, MN 55108, USA; flynn574@umn.edu

[2] Department of Soil and Crop Sciences, Texas A&M University, College Station, TX 77843, USA; k-mcinnes@tamu.edu

* Correspondence: briana.wyatt@tamu.edu

† Work done by K.D. Flynn occurred while an undergraduate at Texas A&M University.

Abstract: Soil moisture is a critical variable influencing plant water uptake, rainfall-runoff partitioning, and near-surface atmospheric conditions. Soil moisture measurements are typically made using either in-situ sensors or by collecting samples, both methods which have a small spatial footprint or, in recent years, by remote sensing satellites with large spatial footprints. The cosmic ray neutron sensor (CRNS) is a proximal technology which provides estimates of field-averaged soil moisture within a radius of up to 240 m from the sensor, offering a much larger sensing footprint than point measurements and providing field-scale information that satellite soil moisture observations cannot capture. Here we compare volumetric soil moisture estimates derived from a novel, less expensive lithium (Li) foil-based CRNS to those from a more expensive commercially available ^{3}He-based CRNS, to measurements from in-situ sensors, and to four intensive surveys of soil moisture in a field with highly variable soil texture. Our results indicate that the accuracy of the Li foil CRNS is comparable to that of the commercially available sensors (MAD = 0.020 m^3 m^{-3}), as are the detection radius and depth. Additionally, both sensors capture the influence of soil textural variability on field-average soil moisture. Because novel Li foil-based CRNSs are comparable in accuracy to and much less expensive than current commercially available CRNSs, there is strong potential for future adoption by land and water managers and increased adoption by researchers interested in obtaining field-scale estimates of soil moisture to improve water conservation and sustainability.

Keywords: cosmic ray neutron sensor; soil moisture; lithium foil

check for updates

Citation: Flynn, K.D.; Wyatt, B.M.; McInnes, K.J. Novel Cosmic Ray Neutron Sensor Accurately Captures Field-Scale Soil Moisture Trends under Heterogeneous Soil Textures. *Water* **2021**, *13*, 3038. https://doi.org/10.3390/w13213038

Academic Editors: Michel Riksen and Zeng-Yei Hseu

Received: 21 September 2021
Accepted: 24 October 2021
Published: 31 October 2021

1. Introduction

Soil moisture is an essential climate variable which influences a number of important hydrological processes, including rainfall infiltration and surface runoff, plant water use, and groundwater recharge, among others [1,2]. A large number of local, regional, and national in-situ soil moisture monitoring networks have been developed around the world in recent years, and the advent of soil moisture remote sensing satellites such as the Soil Moisture Active Passive (SMAP; [3]) and Soil Moisture Ocean Salinity (SMOS; [4]) missions have further increased the availability of soil moisture information [5]. However, despite the increasing availability of soil moisture observations, there remains a gap in the spatial scale between in-situ sensors, which typically measure conditions only within a few centimeters of the sensor itself, and remote sensing observations, which provide a single mean soil moisture value over areas of multiple square kilometers.

The cosmic ray neutron sensor (CRNS) is a technology that has emerged in recent years which can provide field-averaged soil moisture measurements [6]. These sensors bridge the soil moisture measurement spatial scale gap by providing a much larger sensing footprint (i.e., up to a 240-m radius and 0.8-m depth) than point measurements from in-situ sensors [7]. The CRNS is a passive measurement system that relies on incoming primary cosmic ray particles entering the atmosphere and creating cascades of secondary cosmic ray particles, including fast neutrons, that penetrate to the Earth's surface. Because its mass is similar to that of fast neutrons, hydrogen is the most abundant and effective moderator of neutrons, converting fast-moving neutrons to slower neutrons; thus, there is an inverse relationship between fast neutrons and the amount of hydrogen in the environment [7]. Using a site-specific calibration, fluctuations in the number of fast neutrons can be attributed to changes in soil moisture [8].

To measure fast neutron counts, most commercially available CRNSs rely upon ^{3}He and BF_3-filled proportional counting tubes encased in high density polyethylene (HDPE). When fast neutrons enter the tube, ionization occurs and an electric pulse is counted [8,9]. While traditional ^{3}He- or BF_3- based CRNSs meet a critical need in bridging the spatial gap between point measurements and remote sensing soil moisture observations, their adoption outside of the context of scientific research is virtually non-existent, primarily due to the prohibitively high cost of the sensors. Supply for ^{3}He comes from the decay of tritium from nuclear stockpiles, and the limited supply and high demand for ^{3}He has caused prices to continually increase [10]. BF_3-based neutron detectors offer a slightly less expensive alternative, but BF_3 is highly toxic and the cost of BF_3-based CRNSs still limits wider adoption of the technology. However, emerging neutron detection technologies are being developed which significantly decrease the cost of CRNSs [11].

There are several emerging neutron detection technologies that have been field-tested in CRNSs and show promise as replacements of both ^{3}He- and BF_3-based sensors. Recently, a group of researchers in Europe designed a CRNS called Finapp, which utilizes inorganic and plastic scintillators coupled with a photomultiplier for neutron detection. Field testing in Italy and Germany found Finapp to have good agreement with ^{3}He-based CRNSs [12,13]. Another emerging neutron detection technology produced by a group of researchers in Germany and tested for use in CRNSs are boron-lined proportional counters, which have the same measurement principals as commercially available ^{3}He and BF_3 proportional counters [14]. Both Finapp and the boron-lined neutron detection system from Germany can provide additional spectral information on neutrons. This could offer several advantages including the ability to be self-corrected for incoming neutron intensity without relying on external neutron monitoring databases and the potential to distinguishing other hydrogen sources, such as above-ground vegetation biomass, from soil water. While both of these systems are promising replacements for ^{3}He proportional counters, neither are currently commercially available. Radiation Detection Technologies, Inc. (RDT; Manhattan, KS, USA), produces a CRNS using lithium (Li) foil multi-wire proportional counters (MWPC) for neutron detection. These MWPC's contain ^{6}Li metal foils (95% enrichment) suspended between banks of anode wires. Unlike ^{3}He, lithium foils are readily available, as the material is commercially produced by the lithium-ion battery industry [11,15]. Because these materials are more readily available than those used in other types of detectors, they can be produced for 50% or less of the cost of current commercially available sensors. For more detailed information regarding the detector, see the Li-foil neutron detector product page: https://radectech.com/li_foil_neutron.

The measurement theory of CRNSs allows for field-averaged soil moisture estimates to be obtained from a single measurement location. The benefit of this technology is especially evident in heterogeneous environments, where point measurements do not adequately capture field-scale soil moisture dynamics. In environments with heterogeneous soils, CRNSs are likely to be more useful than point measurements for several applications, including long-term modelling of catchment dynamics [16], field-specific irrigation management [17], and for inclusion in land-atmosphere interaction models [8]. The influence of heterogeneous soil types on CRNS readings is highly dependent on the radial distance of the different soil types from the sensor, with areas near the sensor having an exponentially higher impact on neutron readings than areas farther away. For this reason, the relative influence of heterogenous soils on neutron counts and soil moisture derived from CRNS measurements varies as the sensing radius of the CRNS fluctuates [18]. Recently, studies have proposed measuring both fast and slow neutrons to distinguish between near-field and far-field soil moisture dynamics, however the measurement of slow neutrons has not been the focus for monitoring soil moisture [19]. Because CRNS sensing footprints fluctuate in response to changing field conditions, soil moisture heterogeneity near the edge of the field may be excluded during wet seasons when the sensing radius decreases [7]. However, the installation location of CRNSs can be chosen such that near-field heterogeneity is representative of the surrounding area [16].

The objective of this study was to determine whether a novel, less expensive Li foil-based CRNS would perform similarly to a commercially available ^{3}He sensor in providing field-scale estimates of soil volumetric water content, and to evaluate the influence of highly variable soil textures near the edge of the CRNS detection footprint on field-averaged readings as the CRNS sensing footprint fluctuates in response field conditions. Our results indicate (i) that this new Li foil-based CRNS performs nearly identically to the commercially available sensor with respect to estimated soil moisture values and effective sensing radius and depth, and (ii) that both sensors capture the influence of edge-of-field soil textural heterogeneity on soil moisture that is not observed using in-situ point measurements alone. The lower cost of the Li-foil sensor, while still likely prohibitive for applications outside of research, has strong potential for future incorporation into a number of hydrological and agricultural water management scenarios.

2. Materials and Methods

2.1. Site Description

This study was conducted at the Texas A&M University Beef Center in Brazos County (TX, USA) from 3 March to 1 May 2021 (Figure 1A,B). During the study period, the site received 148 mm of precipitation. Mean daily temperatures ranged from 10.3 to 25.4 °C with a mean of 17.6 °C. Mean daily atmospheric pressures ranged from 99.6 to 102.3 kPa with a mean of 100.8 kPa. Mean vapor pressures ranged from 0.7 to 2.6 kPa with a mean of 1.6 kPa. Mean daily absolute humidity ranged from 5.5 to 18.7 g m^{-3} with a mean of 11.5 g m^{-3}.

The land cover within the sensing footprint of the CRNSs was primarily native pasture used for cattle grazing. The soil within a 100-m radius of the neutron detectors was mapped as Ships Clay, a very-fine, mixed, active, thermic Chromic Hapludert ([20], Figure 1C). The edge of the detection area transitioned into Silawa fine sandy loam (fine-loamy, siliceous, semiactive, thermic Ultic Haplustalf) to the north and east and to a Weswood silt loam (fine-silty, mixed, superactive, thermic Udifluventic Haplustpt) to the south and west (Figure 1C). The installation location of the neutron detectors had a cutoff rigidity of 4.63 GeV as calculated by the COSMOS Cutoff Rigidity Calculator (http://cosmos.hwr.arizona.edu/Util/rigidity.php, accessed 15 March 2021).

2.2. Sensors and Installation

2.2.1. Neutron Detectors

Two CRNSs using ^{3}He-filled proportional counting tubes for neutron detection were installed. These CRNSs were manufactured by Hydroinnova LLC (Albuquerque, NM, USA) and designed to be used for both roving and stationary applications. Because these systems were designed to be used for roving applications, they have larger proportional counting tubes and thus a lower measurement uncertainty than a stationary CRNS unit [8]. The ^{3}He-filled proportional counting tubes were housed in 3.7-cm thick high-density polyethylene (HDPE) boxes encased in a steel box for weather protection. These boxes were mounted horizontally on a stand at a height of 0.7 m above the soil surface (Figure 1B). Data loggers for each neutron detector and power supplies were mounted vertically above the neutron detectors and cumulative neutron counts were collected each hour. Due to significant periodic loss of data for one of the ^{3}He CRNS, data from only one ^{3}He CRNS was used for analysis.

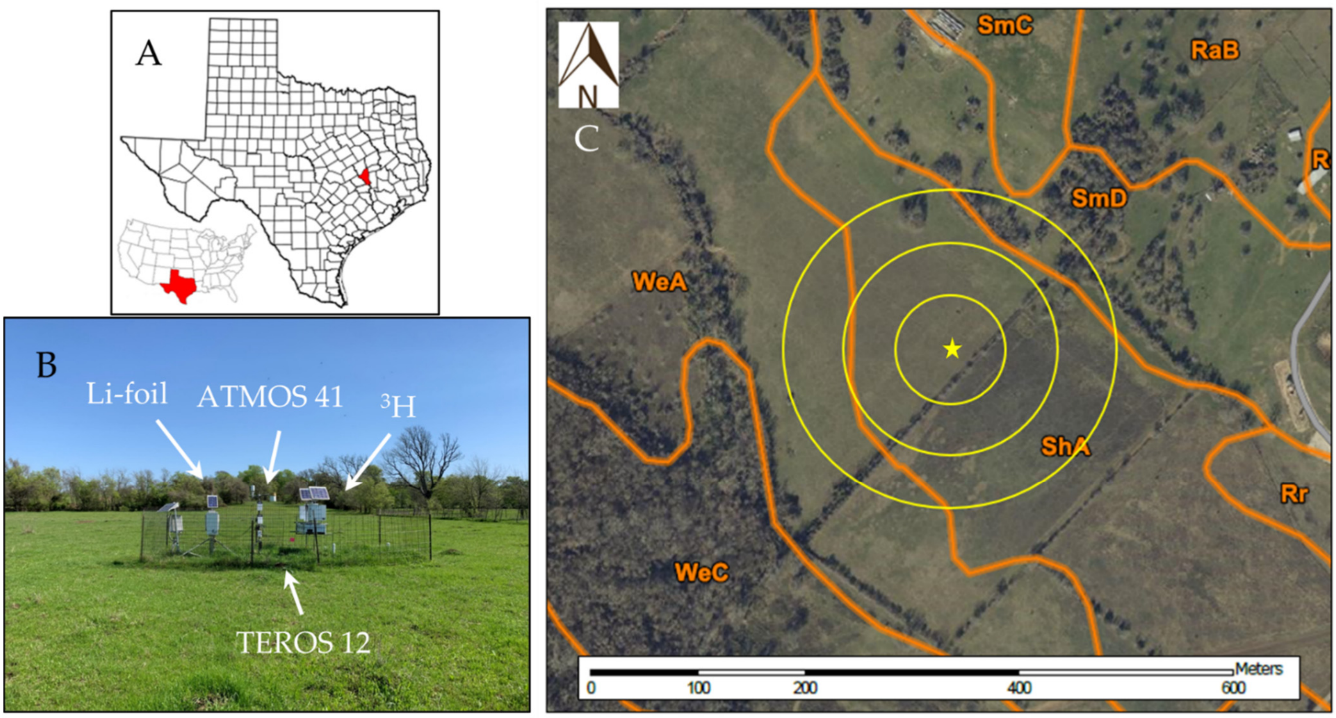

Figure 1. Location of study site in Brazos County, Texas, US (**A**), picture of installed neutron detectors and all-in-one weather station (**B**), and aerial image of the study location, including soil map units and their extents (**C**). Yellow star indicates neutron detector location and yellow circles indicate distances of 50, 100, and 150 m from the detector location. ShA = Ships clay, 0 to 1 percent slopes; WeA = Weswood silt loam, 0 to 1 percent slopes; WeC = Weswood silt loam, 1 to 5 percent slopes; Rr = Roetex clay; SmD = Silawa fine sandy loam, 5 to 8 percent slopes; SmC = Silawa fine sandy loam, 2 to 5 percent slopes; RaB = Rader fine sandy loam, 1 to 3 percent slopes. Image and soil information from NRCS Web Soil Survey [20].

One CRNS consisting of three Li foil multi-wire proportional counters was also installed at the site. This CRNS was manufactured by Radiation Detection Technologies, Inc. (RDT; Manhattan, KS, USA), and it is currently in a beta testing phase. Rather than ^{3}He or BF_3 gas-filled proportional counters, ultra-thin sheets of enriched Li foil are stacked with alternating anode wires between sheets inside of aluminum enclosures [11,15]. The CRNS consists of three Li foil MWPCs insulated with foam and enclosed in a single 2.5-cm thick HDPE box. These neutron detectors were mounted perpendicular to the soil surface, with the center of the detectors at a height of 0.7 m to match the height of the ^{3}He detectors, and each MWPC was wired to a separate channel in a data logger (ZL-6, METER Group, Inc., Pullman, WA, USA). This allowed for modulation of the system in multiple configurations-one where system performance was considered as a sum of cumulative neutron counts from all three Li foil modules, and a second where cumulative neutron counts from individual Li foil modules were considered. Like the ^{3}He detectors, cumulative neutron counts were collected hourly.

2.2.2. Atmospheric Sensors

An ATMOS 41 sensor (METER Group, Inc.) was used to collect atmospheric variables including air temperature, atmospheric pressure, vapor pressure, wind speed and direction, and precipitation at 30-min intervals. A tipping bucket rain gauge was used as a secondary precipitation measurement to supplement precipitation data measured by the ATMOS 41, and any missing measurements from the ATMOS 41 were filled using measurements from the tipping bucket gauge. Precipitation measurements were summed over one-hour intervals, while all other atmospheric measurements were averaged to one-hour intervals in order to match the measurement interval of the CRNSs during data processing.

2.2.3. Soil Moisture Sensors

To provide continuous measurements of soil volumetric water content in the area immediately surrounding the CRNSs, TEROS 12 sensors (METER Group, Inc.) were installed in duplicate (i.e., two sensors per depth) for hourly measurement of volumetric soil moisture, soil temperature, and soil electrical conductivity (EC) at depths of 5 cm, 10 cm, and 20 cm (Figure 1B). These sensors utilized the manufacturer's calibration. Volumetric water content data from these sensors were depth-weighted for comparison with CRNS-estimated volumetric soil moisture by assuming that the mean value of the 5- and 10-cm sensors was representative of the 0–15 cm soil layer and the values reported by the 20-cm sensor were representative of the layer from 15–25 cm.

To measure the spatial variability of soil moisture at the study site and to calibrate the CRNSs, a HydroSense II handheld soil moisture probe (Campbell Scientific, Inc., Logan, UT, USA) was used to conduct four intensive soil moisture surveys ($\overline{n}$ = 154 measurements). The HydroSense is a TDR-type sensor with 12-cm prongs for estimating soil dielectric permittivity and volumetric soil moisture near the soil surface. The sensor was calibrated using volumetric water content measurements from 5.1 cm diameter intact soil cores of 12 cm in length collected in each cardinal direction at 0 m, 50 m, 100 m, and 150 m from the neutron detectors. A calibration equation was then developed by fitting a linear regression between measured volumetric water content from soil cores and the square root of permittivity values measured by the HydroSense (Figure 2). This calibration equation resulted in an RMSE of 0.029 m^3 m^{-3}, indicating an acceptable level of calibration error. Following calibration, distance-weighted mean HydroSense measurements were used to develop a calibration equation for the CRNSs (described in Section 2.4).

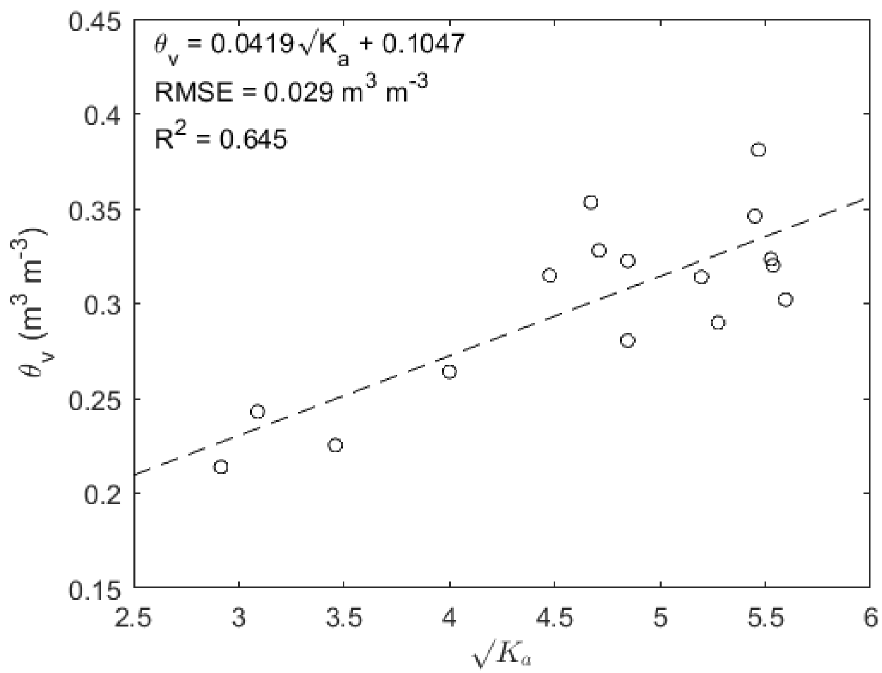

Figure 2. Site-specific calibration equation developed for 0–12 cm HydroSense measurements by relating measured volumetric water content (θ_V) from intact soil cores to the square root of measured dielectric permittivity (K_a) values.

2.3. CRNS Corrections

2.3.1. Correcting Raw Neutron Counts

Prior to analysis, quality control was carried out to remove outliers in raw hourly neutron count readings from both the ^{3}He and the Li foil CRNSs caused by issues with electronics or interference during data retrieval. Outliers were identified as hourly neutron counts greater than the maximum measured hourly neutron count during the driest period of the study.

Raw neutron counts reported by the CRNSs must first be corrected based on incoming neutron intensity and atmospheric conditions that affect neutron movement near the earth's surface, including atmospheric pressure and water vapor pressure. To account for temporal changes in atmospheric pressure, neutron counts were corrected using an exponential atmospheric pressure correction factor [8]. The atmospheric pressure correction factor was calculated using hourly atmospheric pressure measured by the ATMOS 41; a reference pressure of 100.5 kPa, which was determined based on the site elevation; and an atmospheric attenuation coefficient of 0.0075, which was selected based on similarities with sites using the same atmospheric attenuation coefficient in another study [21]. Corrections for atmospheric water vapor content were made based on an atmospheric water vapor correction factor using hourly atmospheric water vapor measurements from the ATMOS 41 [22].

Incoming neutron intensity was accounted for using a correction factor [8]. The JUNG neutron monitoring station (Jungfraujoch, Switzerland, pressure and efficiency corrected) of the Neutron Monitor Database (NMDB, https://www.nmdb.eu/, accessed 15 March 2021) (cutoff rigidity = 4.49 GeV) was used to correct hourly neutron counts for incoming neutron intensity because the JUNG station had the cutoff rigidity nearest that of the study site. The reference neutron intensity was selected as that on 3 March 2021 at midnight, the first evening of the study after CRNS installation.

Raw neutron readings from each CRNS were corrected based on the following equation [21]:

$$N_{corr} = N_{raw}\left(\frac{f_p f_{wv}}{f_i}\right) \quad (1)$$

where N_{corr} is the corrected neutron count, N_{raw} is the uncorrected neutron count logged by the CRNS, f_p is the correction factor for atmospheric pressure, f_{wv} is the correction factor for atmospheric water vapor, and f_i is the correction factor for incoming neutron intensity. Corrected neutron counts were smoothed using a Savitzky-Golay filter with an 11-h window and a third-degree polynomial. This smoothing method was chosen because prior studies have indicated that it adequately preserves peaks associated with precipitation events [23].

2.3.2. Converting Neutron Counts to Volumetric Soil Water Content

Corrected neutron counts were then converted to volumetric soil water content using site-specific soil properties determined from soil samples and independent measurements of volumetric soil moisture from the intensive field surveys. An equation modified from Desilets et al. [24] was used to convert corrected neutron counts to volumetric soil water content, including corrections for lattice water content and soil organic matter [21,25]:

$$\theta_V = \left(\frac{0.0808}{\frac{N}{N_0} - 0.372} - 0.0115 - w_{lat} - w_{SOM}\right)\rho_b \quad (2)$$

where θ_V is neutron-derived field-scale volumetric soil water content [m^3 m^{-3}], N is the corrected neutron count, N_0 is the theoretical neutron count over a dry soil, w_{lat} is lattice water content [g g^{-1}], w_{SOM} is soil organic matter content expressed as a water equivalent [g g^{-1}], and ρ_b is bulk density [g cm^{-3}].

Before converting smoothed, corrected neutron counts to volumetric water content, the N_0 parameter in Equation (2) was defined for each neutron detector by fitting a non-linear least squares regression model to weighted volumetric water content values from the intensive field surveys and 12-h averages of unfiltered, corrected neutron counts including time before, during, and after the field surveys. The sampling strategy of the field surveys is described in the following section.

2.4. Field Surveys for Calibration

A total of four soil moisture surveys were conducted during the study period beginning on 9 April 2021, using the HydroSense II probe to collect point measurements of volumetric soil moisture within the neutron detector footprint. Measurements were taken in each cardinal direction to a distance of 150 m from the CRNSs, with a greater number of measurements near the neutron detectors (Figure 3).

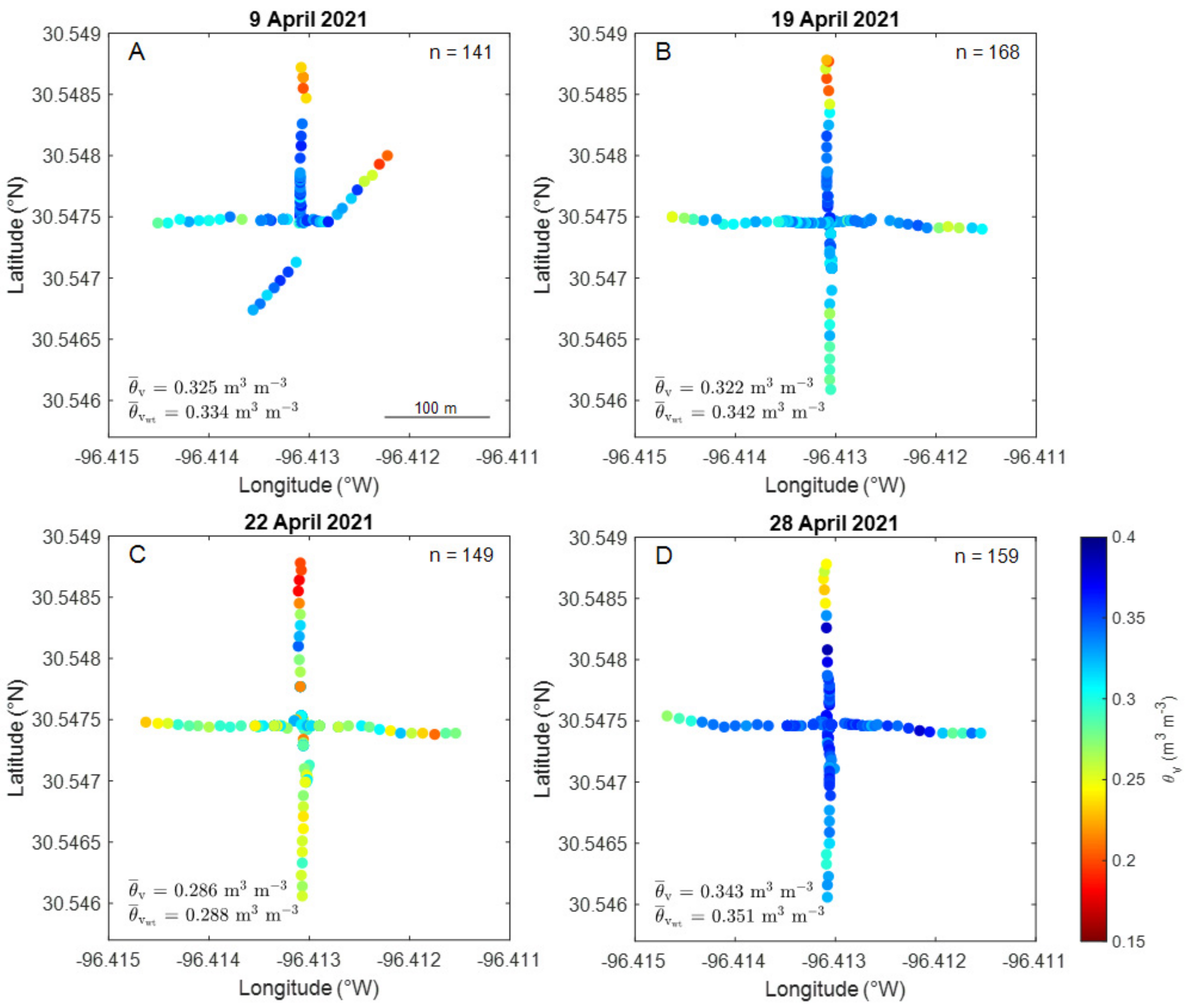

Figure 3. Volumetric water content (θ_V) as measured by the calibrated HydroSense for four intensive field surveys on 9 April 2021 (**A**), 19 April 2021 (**B**), 22 April 2021 (**C**), and 28 April 2021 (**D**). Number of measurement points (n), unweighted mean volumetric water content ($\overline{\theta_v}$), and distance-weighted mean volumetric water content ($\overline{\theta_{v\_wt}}$) shown for each survey date. Initial survey on 9 April followed a different sampling scheme due to restriction of access to private land.

From 0–10 m from the CRNSs, HydroSense readings were taken approximately every 1 m in each direction (~25% of all measurements). From 10–50 m, HydroSense readings were taken approximately every 2 m in each direction (~50% of all measurements). From 50–150 m, HydroSense readings were taken approximately every 10 m in each direction (~25% of all measurements). Overall, approximately 75% of HydroSense readings were taken within a 50-m radius of the neutron detectors during each sampling campaign, with the highest concentration of measurements in the area nearest the detectors. This sampling plan was used because the neutron detectors are especially sensitive to hydrogen sources very near the detectors themselves and less sensitive to sources at greater distances [7].

During the 9 April and 19 April sampling campaigns, a total of 21 soil cores were collected to a depth of 12 cm at 0 m, 50 m, 100 m, and 150 m in each cardinal direction from the center point between the neutron detectors. Cores were collected at each distance in the west and south directions on 19 April only due to lack of access to private land on the first sampling date. Otherwise, one sample was collected at each distance in all directions on each sampling date. Each soil core was collected at approximately the same time as the HydroSense reading was taken at the given location in order that sensor readings would correspond to sample collection for calibration of the HydroSense. Each soil core was oven dried at 105 °C for 24 h to calculate gravimetric water content and bulk density ($\overline{\rho_b}$ = 1.20 g cm^{-3}). Measured volumetric water content values from 16 of the soil cores were used to create a site-specific calibration of the HydroSense using a linear regression between soil core volumetric water content and HydroSense dielectric permittivity readings (Figure 2). Five cores were excluded from the HydroSense calibration procedure due to the inclusion of rock fragments or incomplete sample volumes.

Each soil sample collected was also analyzed to determine soil texture (Table 1), and composite subsamples of soil from the 50 and 100 m sampling distances were analyzed for soil organic matter ($\overline{\mathrm{SOM}} = 2.02\%$) and lattice water content ($\overline{w_{\mathrm{lat}}}$ = 0.028 g g^{-1}) to account for static pools of hydrogen within the CRNS footprint. To determine whether vegetation water content had a significant impact on neutron counts, three vegetation samples were also collected at random locations within the sensing footprint and were analyzed to determine dry above-ground biomass. These samples had an average dry above-ground biomass of 0.299 kg m^{-2} (σ = 0.176 kg m^{-2}). Prior work by Baatz et al. [26] has indicated that a dry above-ground biomass of ~1.0 kg m^{-2} should be accounted for by reducing neutron counts by 0.9%. Because dry above-ground biomass at our site was much lower than that given by Baatz et al. [26], the effect of vegetation was assumed to be negligible for our study site.

Table 1. Sand and clay percentage and soil textural class of soil samples collected in the center of the field, at 100 m, and at 150 m from the neutron detectors in each cardinal direction. SiCL = city clay loam, CL = clay loam, SiL = silt loam, LS = loamy sand, SCL = sandy clay loam.

Location	Sand %	Clay %	Textural Class –
Center	18.8	31.2	SiCL
North 100 m	35.7	28.7	CL
East 100 m	25.0	37.5	CL
South 100 m	15.7	27.5	SiCL
West 100 m	16.6	26.9	SiL
North 150 m	81.5	5.0	LS
East 150 m	47.5	27.5	SCL
South 150 m	17.5	25.0	SCL
West 150 m	25	17.5	SiL

2.5. Sensing Footprint

Prior to calibration of the CRNSs, each HydroSense survey point was assigned a radial weight using a radial weighting function [7]. The weighting values, which are dependent on soil moisture and absolute humidity, were assigned based on un-weighted field-averaged volumetric water content of each intensive survey and absolute humidity during each survey. The weighted field-averaged values were then used to calibrate the CRNSs. Because the HydroSense provides a single volumetric water content value for the top 12 cm of the soil profile, no depth weighting of survey points was applied.

The effective radial sensing footprint, R_{86}, and effective depth of measurement, D_{86}, for each CRNS are defined as the radial distance from which 86% of detected neutrons originate and the depth from which 86% of detected neutrons originate, respectively [7]. The effective radial sensing footprint was manually computed for the time period when each HydroSense survey was performed using the weighted field-averaged volumetric water content value from the survey and the average absolute humidity measured during the survey. Theoretical maximum effective radial sensing footprints were also calculated for both CRNSs using the maximum estimated volumetric water content from each sensor during the study period and the maximum absolute humidity measured during the study period. Theoretical minimum effective radial sensing footprints were estimated in the same way using minimum volumetric water content and absolute humidity values. The effective sensing depth was computed daily for each date in the study period using mean volumetric water content estimates from each CRNS and daily mean absolute humidity values.

Analysis of CRNS, TEROS 12, and ATMOS 41 data was performed in Python using the Matplotlib, numpy, pandas and scipy packages [27–30]. Analysis and calibration of HydroSense II measurements was done using MATLAB (2021a, The MathWorks, Inc., Natick, MA, USA).

3. Results and Discussion

3.1. Field Site Characteristics

Soil cores collected at radial distances of 0 m, 50 m, 100 m, and 150 m, in each cardinal direction from the CRNSs were used to characterize the soil properties of the field. Table 1 displays soil texture analysis from soil cores collected throughout the field. Soil texture at 0 m from the CRNS was a silty clay loam (SiCL). Soil textures at 100 m from the CRNSs included clay loam (CL), silty clay loam (SiCL), and silt loam (SiL). Soil textures at 150 m from the CRNS included loamy sand (LS), sandy clay loam (SCL) and silt loam (SiL). These soil textural classes are indicative of the high level of soil texture variability of the field; measured sand contents ranged from <16% to >80% and clay contents ranging from 5% to nearly 40% (Table 1).

3.2. Calibration

Due to the high clay content of the soil at the study site, especially near the neutron detectors, it was necessary to develop a site-specific calibration of the HydroSense probe used for intensive soil moisture surveys. The square root of the apparent dielectric permittivity of the HydroSense probe was linearly related to the volumetric water content (Figure 2), with $R^2 = 0.645$ and RMSE = 0.029 $m^3 m^{-3}$ for volumetric water contents ranging from 0.21 to 0.38 $m^3 m^{-3}$. The level of error associated with the HydroSense calibration is comparable to similar calibrations developed in prior studies (e.g., [25,31]) and is less than the value of 0.032 $m^3 m^{-3}$ found by Patrignani et al. [32], who used a calibrated HydroSense probe for comparison with volumetric water content estimates from the same type of Li foil neutron detector used in the present study.

Distance-weighted field-average volumetric soil moisture estimates resulting from HydroSense surveys ranged from 0.286 to 0.343 $m^3 m^{-3}$ and within-survey variations of weighted mean volumetric water content values ranged from 0.015 to 0.033 $m^3 m^{-3}$ (Table 2). The greatest variations in soil moisture measured by the HydroSense occurred near the western, northern, and eastern edges of the survey radius, where soils shifted from clay-dominated to sandy soils (Figure 1c, Table 1). This change in soil texture is clearly reflected in the HydroSense readings, with the greatest change in soil moisture levels occurring in the northernmost portion of the field where soils abruptly transition to a loamy sand with 81.5% sand content. This trend was observed in all four field surveys but is most evident during the field survey on 28 April, when high volumetric water contents were measured in the clay-dominated soils near the CRNSs. During this same survey, the surface horizon of the sand-dominated soil in the northeast portion of the field was already well drained. (Figure 3, Table 1).

Table 2. Number of observations (n), mean unweighted volumetric water content ($\overline{\theta_v}$) of HydroSense surveys, mean weighted volumetric water content ($\overline{\theta_{v\_wt}}$) of HydroSense surveys, mean absolute humidity ($\overline{AH}$) during the time of sampling, and the effective CRNS sensing radius (R_{86}). Standard deviations are shown in parentheses.

Date	n	$\overline{\theta_v}$ $m^3\ m^{-3}$	$\overline{\theta_{v\_wt}}$ $m^3\ m^{-3}$	$\overline{AH}$ $g\ m^{-3}$	R_{86} m
9 April 2021	141	0.325 (0.035)	0.334 (0.021)	16.2 (0.516)	140
19 April 2021	168	0.322 (0.029)	0.342 (0.015)	10.2 (0.348)	151
22 April 2021	149	0.286 (0.035)	0.288 (0.033)	11.0 (0.222)	154
28 April 2021	159	0.343 (0.026)	0.351 (0.014)	19.7 (0.303)	135

Distance-weighted mean volumetric water content data from these field surveys and measured soil property information were used to develop site-specific calibrations for the CRNSs (Table 2, Figure 4). The calibrations for the Li foil and ^{3}He CRNSs indicate a good agreement with the HydroSense surveys with R^2 = 0.82 and R^2 = 0.90, respectively. While the driest period of the study was well characterized by the HydroSense survey on 22 April periods of high volumetric water content immediately following precipitation events were not captured by the surveys due to accessibility issues in the heavy clay soils at the site when wet. However, the calibration points captured by the field surveys are adequate as indicated by the high coefficient of determination (R^2) values for the calibrations (Figure 4). Further, it has been demonstrated that the most accurate CRNS calibrations are achieved when calibration sampling includes dry conditions, similar to those captured during the driest field survey shown here, due to the increased sensitivity of the detectors at low soil water contents ([18,33], Figure 4).

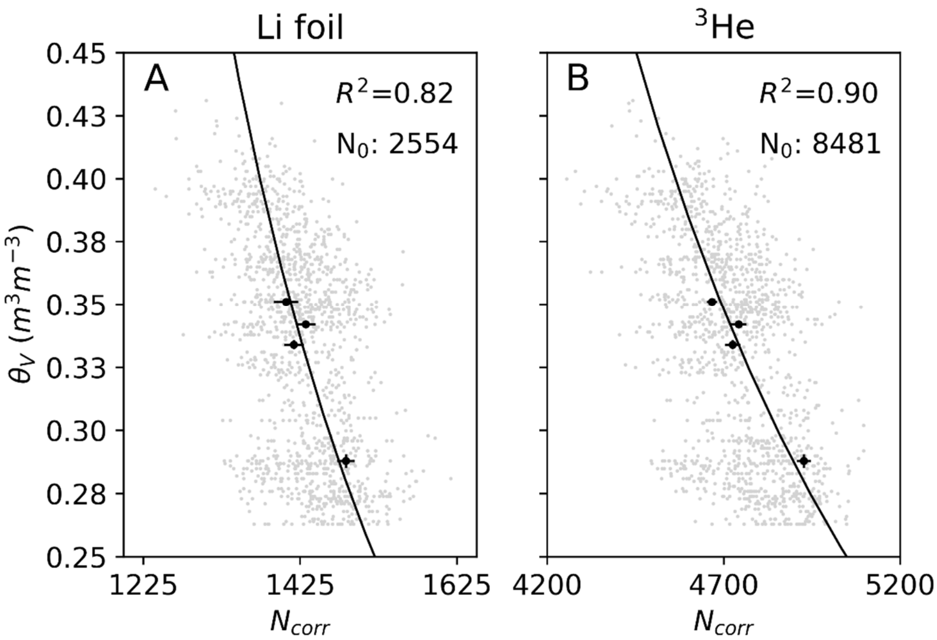

Figure 4. Calibration curve of Li foil (**A**) and ^{3}He (**B**) CRNSs developed using distance-weighted field average volumetric water content (θ_V) data from four intensive field surveys. Corrected, unfiltered hourly neutron counts (N_{corr}) representing a 12-h period including time before, during, and after the field surveys were used for calibration. Error bars represent the standard error of the mean. Grey points represent hourly readings from profile of TEROS 12 sensors and are included to show range of θ_V values but were not used to develop calibration equation.

Characterizing the spatial distribution of soil moisture within the study site using intensive soil moisture surveys was especially important in this study because of the sharp soil moisture gradients caused by abrupt soil textural changes. The profile of in-situ soil moisture sensors installed near the CRNSs represent conditions only near the detectors, and indeed, point-scale soil moisture trends captured by these sensors vary substantially from those of the CRNSs, particularly during drying events; thus, these sensors did not capture the spatial variability necessary to be useful for calibration of the CRNSs. Conversely, using the HydroSense to conduct multiple, intensive field surveys allowed for faster measurement and higher spatial coverage as compared to other CRNS calibration methods such as intensive soil sampling for oven-dry determination of soil water content or installation of permanent arrays of in-situ soil moisture sensors [21,34,35]. The identification of soil and hydrologic transition zones within the field was important for understanding how variations in soil water content influenced CRNS readings, which was especially important in our study since soil water content decreased by as much as 45% from the location of the CRNSs to the edge of the sensing footprint.

3.3. Corrected Neutron Counts

The uncertainty of CRNS measurement is dependent on site and detector characteristics. The neutron count rate (N) obeys Poisson statistics where the coefficient of variation is estimated using $N^{-0.5}$ [8,36]. As conditions that influence the neutron count rate change, such as soil moisture content, the measurement variation will also change. This uncertainty is also affected by the design and size of the neutron detector module and by changes in the time period over which neutron count rates are summed [8]. There is a greater uncertainty associated with corrected neutron counts for the sum of all three Li foil modules (2.65%) as compared to the ^{3}He sensor (1.45%) (Table 3). This difference in uncertainty is due to the greater size- and therefore higher count rate- of the ^{3}He neutron detector, which was designed for dual use as a roving and a stationary unit.

Table 3. Mean uncorrected hourly neutron counts ($\overline{N_{uncorr}}$), mean corrected hourly neutron counts ($\overline{N_{corr}}$), device-specific calibration parameter (N_0), uncertainty of corrected hourly neutron counts ($N^{-0.5}$), 11-h moving coefficient of variation of volumetric water content estimated by CRNS (CV). All values represent measurements over a period of 1391 h.

	$\overline{N_{uncorr}}$ Counts h^{-1}	$\overline{N_{corr}}$ Counts h^{-1}	N_0 Counts h^{-1}	$N^{-0.5}$ %	CV %
Li foil 1	445	483	879	4.5	8.4
Li foil 2	463	503	889	4.5	7.9
Li foil 3	406	441	782	4.8	7.6
All Li foil	1315	1427	2554	2.6	4.9
^{3}He	4360	4730	8481	1.5	3.8

When considering a single Li foil module, the measurement uncertainty was as great as 4.76%, and measurement uncertainty decreased as the number of modules increased (Table 3). Depending on the user application, using a system with less than three Li foil neutron detectors could be acceptable. For example, in Patrignani et al. [32] uncertainty in corrected hourly neutron counts for the sum of all three Li foil neutron detectors was 2.25%, and uncertainty of a single Li foil neutron detector was 4.01%. Because of differences in site characteristics between the two studies (i.e., greater soil and atmospheric water contents), the measurement uncertainty of the Li foil CRNS was slightly higher here than in Patrignani et al. [32].

3.4. Normalized Neutron Counts

Because the ^{3}He CRNS is designed for use as a rover, its raw neutron count rate is much higher than that of the Li foil sensor. Therefore, this study is not a comparison of two equivalent systems such as in Patrignani et al. [32]. For this reason, a comparison of normalized neutron counts between the ^{3}He CRNS and the Li foil CRNS provides the best means of comparing the performance of the different neutron detectors used in each system.

Throughout the study, normalized neutron counts from the Li foil and ^{3}He neutron detectors reacted similarly to changing field conditions (Figure 5). There are periods where normalized neutron counts of both CRNSs gradually increase through time until a sharp decrease. This is indicative of soil within the CRNS sensing footprint gradually drying until a precipitation event causes soil moisture to quickly increase. While the greater variation of the Li foil CRNS compared to the ^{3}He CRNS is evident by the higher peaks and lower troughs, the response to changing field conditions (i.e., soil drying and soil wetting) is consistent between both CRNSs throughout the duration of the study.

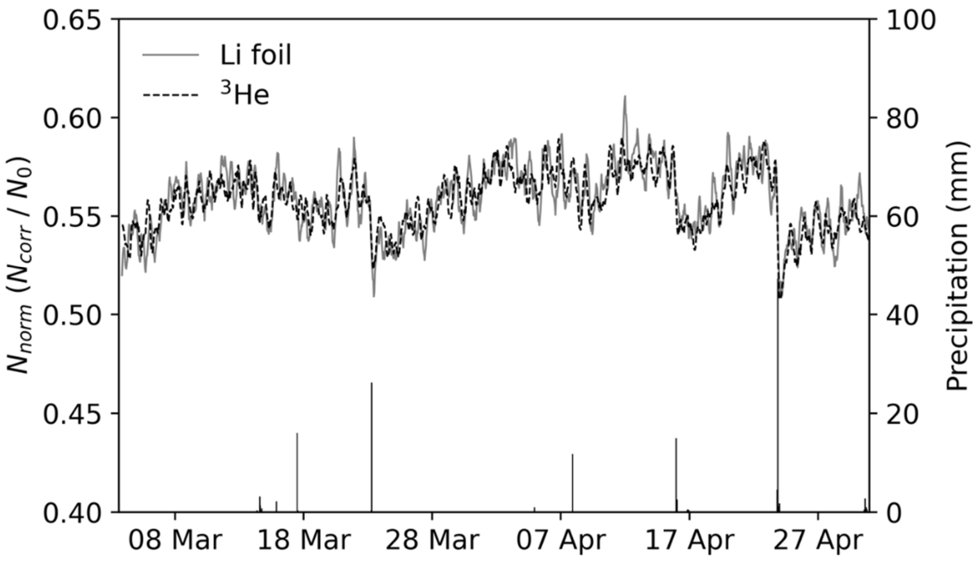

Figure 5. Time series of normalized corrected neutron counts (N_{norm}) of Li foil and ^{3}He CRNSs throughout the duration of the study period. Corrected neutron counts were smoothed using a Savitzky-Golay filter (11-h window, third-degree polynomial).

There is a moderately strong correlation between normalized corrected neutron counts from the Li foil and ^{3}He CRNSs (R^2 = 0.72, Figure 6). As can be seen in Figure 6, the disagreement in normalized neutron counts between the two sensors is greatest during and immediately following precipitation events, when normalized neutron counts were lowest. During these times, the Li foil CRNS reported a greater response than the ^{3}He CRNS to the increased level of water in the environment. A similar pattern was observed by Patrignani et al. [32], though to a lesser degree. The observed difference in normalized neutron counts is likely explained by the lower measurement uncertainty of the ^{3}He CRNS *as* compared to that of the Li foil sensor. The measurement uncertainty is exponentially and inversely proportional to the number of neutron counts, meaning that the greater uncertainty associated with the Li foil CRNS would be most apparent at the wettest conditions, which is the case in this study.

3.5. Sensing Footprint

The heterogeneous soil near the edge of the field and the wide range of soil moisture and absolute humidity conditions throughout the study required any interpretation of our data to rely heavily on a knowledge of the range of the neutron detector's effective horizontal sensing radius. During the study period the effective horizontal sensing radius of the CRNS varied by up to 24%. The effective horizontal sensing radius (R_{86}) is the estimated area from which 86% of the measured neutrons are derived, and is estimated by solving the following equation numerically:

$$\int_0^{R_{86}} W_r d_r = 0.86 \int_0^{\infty} W_r d_r$$

where W_r is the detected neutron intensity [7].

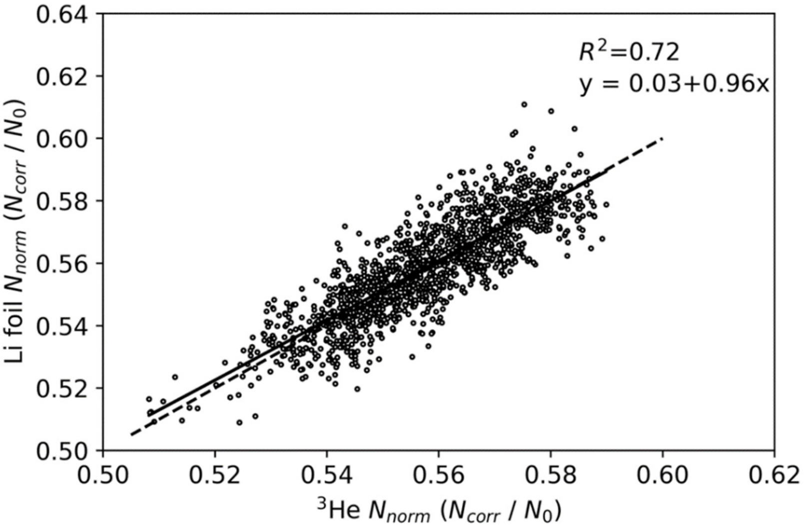

Figure 6. Scatterplot of normalized corrected neutron counts (N_{norm}) of ^{3}He and Li foil CRNS throughout the duration of the study period. The dashed line is the 1:1 line and the solid line is the line of best fit. Corrected neutron counts were smoothed using a Savitzky-Golay filter (11-h window, third-degree polynomial).

Based on weighted field-averaged volumetric water content measured by the CRNSs and relative humidity measurements, the maximum effective horizontal sensing radius of the neutron detectors during field surveys ranged from 135 to 154 m, indicating that our HydroSense measurements captured a comparable horizontal area and range of soil moisture conditions as the neutron detectors during the periods when surveys were conducted (Table 3). However, the effective horizontal sensing footprint likely fluctuated beyond this range, because soil moisture and absolute humidity maximum and minimums during the study period did not occur during the times when field surveys were conducted. Considering the maximum volumetric water content measured by both CRNSs and the maximum absolute humidity during the study period, which did not occur simultaneously, the minimum possible sensing footprint for both the Li foil and the ^{3}He CRNS would have been 133 m. Considering the minimum field-average volumetric water content measured by both CRNSs and the minimum absolute humidity during the study period, which did not occur simultaneously, the maximum possible sensing footprints for the Li foil and the ^{3}He CRNS would have been 175 m and 168 m, respectively. During wet and humid conditions, when the horizontal sensing radius was smaller, the influence of drier, sandy soils near the edge of the field on CRNS readings was likely low. Conversely, during dry conditions, when the sensing radius increased, those same soils had a greater influence on CRNS readings.

The impact of the CRNS's larger sensing radius on soil moisture estimates becomes apparent when CRNS volumetric water content estimates are compared with the TEROS 12 volumetric water content measurements, which are representative of soil moisture levels only in the clay soil near the center of the field. During the first weeks of the study, a dry-down period occurs prior to the first precipitation event. During this period, the CRNS volumetric water content estimates are lower than the TEROS 12 depth-weighted mean volumetric water content values. This occurs because the TEROS 12 sensors are only influenced by the high clay soils directly around the sensors, which retain water longer than sandy soils, while the CRNS measurements are influenced by regions much further from the detectors, including those near the edge of the field that have higher sand contents and lower soil water contents than the center of the field (Figure 3). Because the CRNS sensing radius (R_{86}) increases as soil water content decreases, the influence of the sandy soils near the edge of the field were more influential the drier the site became.

Like the effective sensing radius, the effective sensing depth (D_{86}) of the CRNSs also varies depending upon the amount of water in the surrounding environment. D_{86} values for both CRNSs ranged from 14 cm during the wettest conditions at 150 m from the sensors to 26 cm during the driest conditions at 0 m from the sensors (Figure 7). Figure 7 shows how daily mean effective sensing depths varied with soil moisture for the Li foil and ^{3}He CRNS at 0 m from the sensors and at 150 m from the sensors. These results indicate that the HydroSense, which had 12 cm rods, did not provide measurements to the full depth of influence for CRNS readings. However, other studies using hand-held sensors for calibration have achieved adequate calibrations sampling shallower than the sensing depth of the CRNS [25,31,32]. Our study relies on similar assumptions that the influence of soil moisture on CRNS measurements at greater depths than our field survey sampling is not significant enough to significantly influence the calibrations developed. This is supported by data from the profile of TEROS 12 sensors, which reported mean volumetric water content values during the study period of 0.319 m^3 m^{-3} at 5 cm, 0.343 m^3 m^{-3} at 10 cm, and 0.334 m^3 m^{-3} at 20 cm. In fact, *t*-tests indicate that there was a significant difference between daily mean TEROS 12 volumetric water content measurements at 5 and 10 cm ($t[58] = -3.1$, $p = 0.002$) but not between daily mean TEROS 12 volumetric water content measurements at 10 and 20 cm ($t[58] = 1.1$, $p = 0.294$). This indicates that the majority of soil moisture variations occurred near the surface, where the effects of rainfall, soil water evaporation, and plant water uptake are most concentrated, and supports the claim that HydroSense measurements captured the majority of the soil moisture variation with depth that was also captured by the CRNSs.

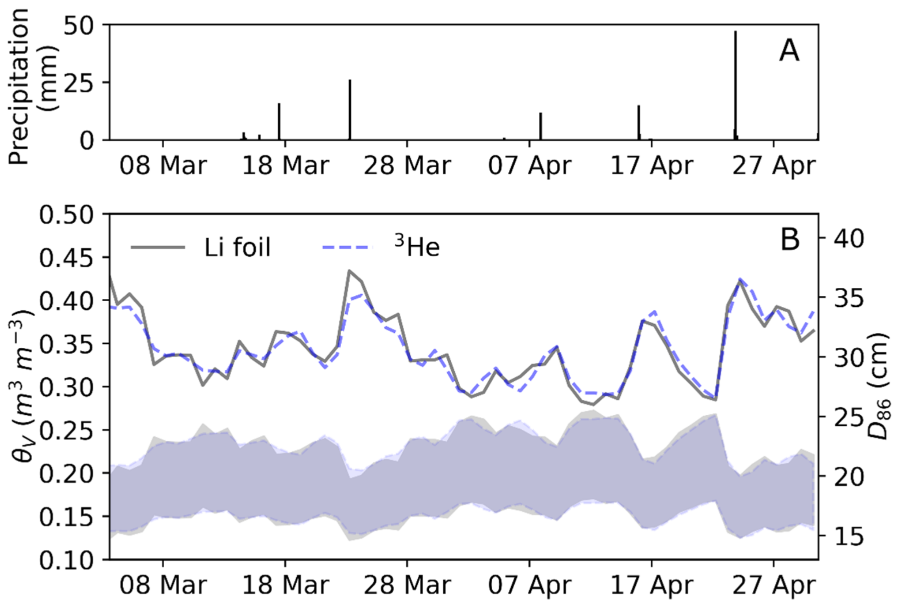

Figure 7. Daily precipitation during the study period (**A**) and daily mean Li foil CRNS volumetric water content (θ_V, gray line), daily mean ^{3}He CRNS volumetric water content (blue line), and range in effective sensing depth (D_{86}) of Li foil (gray shaded region) and ^{3}He (blue shaded region) CRNSs (**B**). The range in effective sensing depth is bounded by the effective sensing depth at 0 m (upper limit of shaded region) and 150 m (lower limit of shaded region) based on daily average volumetric water content from CRNSs and daily mean absolute humidity.

3.6. CRNS-Derived Soil Moisture

The main objective of our study was to evaluate the ability of a novel Li foil CRNS to provide accurate field-scale estimates of soil moisture. The mean absolute difference (MAD) was used to quantify differences in measured and estimate volumetric water content between sensors considered in this study (Table 4). The MAD between volumetric soil moisture estimates from the Li foil CRNS and ^{3}He CRNS was low (MAD = 0.020 m^3 m^{-3}) and comparable to the value of 0.017 m^3 m^{-3} reported by Patrignani et al. [32] who tested the same type of Li foil CRNS used here against a BF_3 CRNS. The MAD between the depth-weighted volumetric water content from the profile of TEROS 12 sensors and the ^{3}He CRNS was 0.031 m^3 m^{-3} and the MAD between the profile of TEROS 12 sensors and the Li foil CRNS was 0.032 m^3 m^{-3}. The lower MAD value seen between the CRNSs as compared to that found between each CRNS and the TEROS 12 sensors is to be expected due to the discrepancy between the CRNSs' measurement radius and the much smaller measurement volume of the TEROS 12 sensors. Furthermore, the CRNSs measured unrealistically high peaks in volumetric water content (i.e., >0.50 m^3 m^{-3}) during and immediately after precipitation events (Figure 7), which is indicative of the measurement of precipitation itself and/or temporary ponding within the footprint of the CRNS. This observation is also reported by prior studies [5,8]. This overestimation of soil volumetric water content during precipitation events contributed to the greater MAD between each CRNS and the profile of TEROS 12 sensors. Regardless, the similarity in MAD between the ^{3}He CRNS and TEROS 12 profile and between the Li foil CRNS and TEROS 12 profile provides strong evidence that the less expensive Li foil CRNS is comparable to and a viable alternative to costly ^{3}He CRNSs.

Table 4. Mean absolute difference (MAD) of volumetric water content between sensors during the study period. Volumetric water content estimates from CRNSs were calculated using corrected neutron counts smoothed with Savitsky-Golay filter (11-h window, third-degree polynomial).

Sensors	MAD m^3 m^{-3}
Li foil vs. ^{3}He	0.020
Li foil vs. TEROS 12	0.032
^{3}He vs. TEROS 12	0.031

When comparing the CRNSs' estimates of volumetric water content, the inherent measurement uncertainty of each sensor must be considered. The ^{3}He CRNS has a higher hourly neutron count rate than the Li foil CRNS, so the measurement precision is higher than that of the Li foil CRNS. Volumetric water content will also be less variable for the ^{3}He CRNS than for the Li foil CRNS. The 11-h moving coefficient of variation of volumetric water content estimates is 3.8% for the ^{3}He CRNS and 4.9% for the Li foil CRNS (Table 3). The 11-h moving coefficient of variation for soil volumetric moisture estimates from each individual Li foil modules ranges from 7.6% to 8.4% (Table 3). The difference in variation between the individual Li foil units and the sum of all three Li foil units is much greater than the difference in variation between the sum of all three Li foil units and the ^{3}He CRNS due to the non-linear relationship between measurement uncertainty and neutron count rate ($N^{-0.5}$).

It should be noted that after a rain event on 16 April, the difference in volumetric water content as measured by the CRNSs and the TEROS 12 profile is significantly greater than at any other point during the study. During the rain event on 15 April, ATMOS 41 wind measurements indicate that strong winds and heavy rain were interfering with the transducers used for wind speed measurement. Before wind speed and direction measurements went offline, the predominant wind direction was from the east. Because of the configuration of the test bed (Figure 1), a strong wind from the east during a heavy rain event would cause the ^{3}He neutron detectors to shield the profile of TEROS

12 sensors below from precipitation falling at an ~45° angle. This shielding likely prevented precipitation from falling directly on the soil above the TEROS 12 sensors, leading to a much lower increase in soil moisture than would be expected based on a comparison of the sensors to other rainfall events of a similar magnitude (Figure 8).

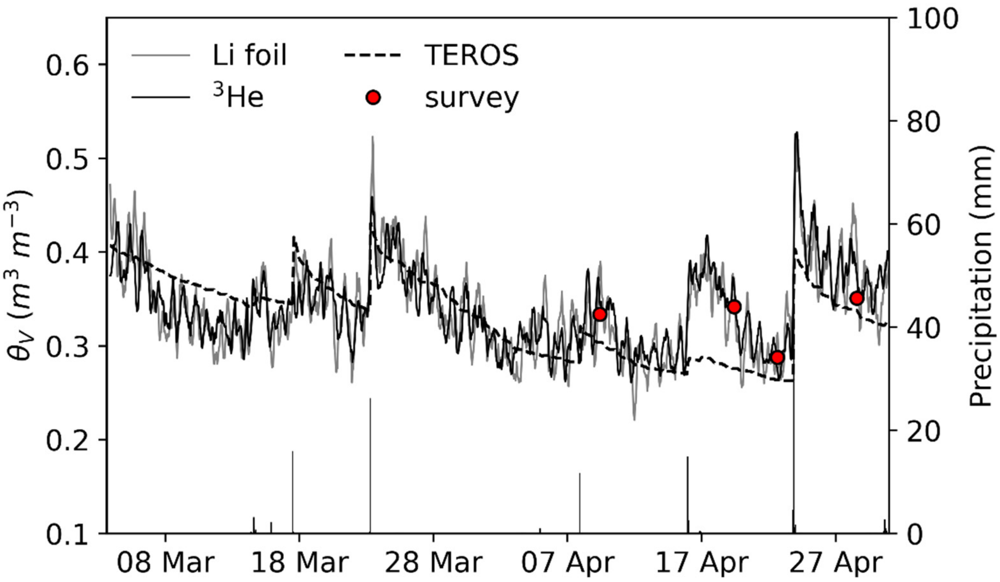

Figure 8. Volumetric water content (θ_V) estimated from Li foil and ^{3}He CRNS measurements, profile of TEROS 12 sensors, and four intensive field surveys and precipitation throughout duration of study period.

4. Conclusions

In this study, we compared estimates of volumetric soil moisture derived from a novel, lower cost Li foil CRNS with those from a more expensive, commercially available ^{3}He CRNS. We also show that this novel Li foil CRNS provides information on field-average soil moisture conditions that point estimates from in-situ sensors cannot capture. Measurements from the CRNSs agreed well, with a MAD in volumetric water content of 0.020 m^3 m^{-3}. Additionally, the sensing radius and depth of the CRNSs were similar, indicating that the less expensive Li foil detector used here is a viable alternative to currently available commercial sensors, which can cost upwards of $15,000. This lower-cost alternative, while still likely cost-prohibitive for personal use, has strong potential to improve the adoption of CRNSs for soil moisture measurement and water management applications by land managers and the scientific community.

As other studies have indicated the placement of CRNS in heterogeneous conditions must be carefully considered to capture average volumetric water content representative of the broader field conditions. In our study, the effect of soil heterogeneity near the edge of the CRNS detection area was evident throughout the entirety of the study, though to differing degrees in wet and dry conditions. However, our study only represents a portion of the temporal variability in field soil moisture conditions at this site, and the area influencing the CRNS could differ greatly throughout the year, which could affect interpretations of field-scale soil moisture dynamics.

Supplementary Materials: The following are available online at https://www.mdpi.com/article/10.3390/w13213038/s1, Data S1: Hourly data from the CRNSs, TEROS 12 sensors, and ATMOS 41 presented in this manuscript. Data S2: HydroSense data from four field surveys used to characterize field soil moisture conditions and to calibrate the CRNSs.

Author Contributions: Conceptualization, methodology, writing—review and editing, K.D.F., B.M.W., K.J.M.; Formal analysis, visualization, writing—original draft, K.D.F., B.M.W. All authors have read and agree to the published version of the manuscript.

Funding: This research received no external funding.

Data Availability Statement: The data presented in this study are available in supplementary material.

Acknowledgments: We acknowledge the NMDB database (www.nmdb.eu, accessed 15 March 2021) founded under the European Union's FP7 program (contract no. 213007), and the PIs of individual neutron monitoring sites at: IGY Jungfraujoch (Physikalisches Institute, University of Bern, Switzerland). We also acknowledge Texas A&M AgriLife Research for managing the field site used in this study.

Conflicts of Interest: The authors declare no conflict of interest.

References

1. Wagner, W.; Blöschl, G.; Pampaloni, P.; Calvet, J.C.; Bizzarri, B.; Wigneron, J.P.; Kerr, Y. Operational readiness of microwave remote sensing of soil moisture for hydrologic applications. *Hydrol. Res.* **2007**, *38*, 1–20. [CrossRef]
2. Wagner, W.; Dorigo, W.; de Jeu, R.; Fernandez, D.; Benveniste, J.; Haas, E.; Ertl, M. Fusion of active and passive microwave observations to create an essential climate variable data record on soil moisture. *ISPRS Ann. Photogram. Remote Sens. Spat. Inf. Sci.* **2012**, *I-7*, 315–321. [CrossRef]
3. Entekhabi, D.; Njoku, E.G.; O'Neill, P.E.; Kellogg, K.H.; Crow, W.T.; Edelstein, W.N.; Entin, J.K.; Goodman, S.D.; Jackson, T.J.; Johnson, J.; et al. The soil moisture active passive (SMAP) mission. *Proc. IEEE* **2010**, *98*, 704–716. [CrossRef]
4. Kerr, Y.H.; Font, J.; Martin-Neira, M.; Mecklenburg, S. ESA's soil moisture and ocean salinity mission (SMOS)-instrument performance and first results. *Trans. Geosci. Remote Sens.* **2012**, *50*, 1351–1715. [CrossRef]
5. Ochsner, E.; Cosh, M.H.; Cuenca, R.H.; Dorigo, W.A.; Draper, C.S.; Hagimoto, Y.; Kerr, Y.H.; Larson, K.M.; Njoku, E.G.; Small, E.E.; et al. State of the art in large-scale soil moisture monitoring. *Soil Sci. Soc. Am. J.* **2013**, *77*, 1888–1919. [CrossRef]
6. Zreda, M.; Desilets, D.; Ferré, T.P.A.; Scott, R.L. Measuring soil moisture content non-invasively at intermediate spatial scale using cosmic-ray neutrons. *Geophys. Res. Lett.* **2008**, *35*, L21402. [CrossRef]
7. Köhli, M.; Schrön, M.; Zreda, M.; Schmidt, U.; Dietrich, P.; Zacharias, S. Footprint characteristics revised for field-scale soil moisture monitoring with cosmic-ray neutrons. *Water Resour. Res.* **2015**, *51*, 5772–5790. [CrossRef]
8. Zreda, M.; Shuttleworth, W.J.; Zeng, X.; Zweck, C.; Desilets, D.; Franz, T.; Rosolem, R. COSMOS: The cosmic-ray soil moisture observing system. *Hydrol. Earth Sys. Sci.* **2012**, *16*, 4079–4099. [CrossRef]
9. Krane, K.S.; Halliday, D. *Introductory Nuclear Physics*; John Wiley & Sons, Inc.: New York, NY, USA, 1988; pp. 204–206.
10. Kouzes, R.T. *The ^{3}He Supply Problem*; Report No. PNNL-18388; Pacific Northwest National Lab (PNNL): Richland, WA, USA, 2009.
11. Nelson, K.A.; Bellinger, S.L.; Montag, B.W.; Neihard, J.L.; Riedel, T.A.; Schmidt, A.; McGregor, D.S. Investigation of a lithium foil multi-wire proportional counter for potential ^{3}He replacement. *Nucl. Inst. Meth. Phys. Res. Sec. A Accel. Spectrometers Detect. Assoc. Equip.* **2012**, *669*, 79–84. [CrossRef]
12. Stevanato, L.; Baroni, G.; Cohen, Y.; Fontana, C.L.; Gatto, S.; Lunardon, M.; Marinello, F.; Moetto, S.; Morselli, L. A novel cosmic-ray neutron sensor for soil moisture estimation over large areas. *Agriculture* **2019**, *9*, 202. [CrossRef]
13. Stevanato, L.; Polo, M.; Lunardon, M.; Marinello, F.; Moretto, S.; Baroni, G. Towards the optimization of a scintillator-based neutron detector for large non-invasive soil moisture estimation. In Proceedings of the 2020 IEEE International Workshop on Metrology for Agriculture and Forestry (MetroAgriFor), Trento, Italy, 4–6 November 2020. [CrossRef]
14. Weimar, J.; Köhli, M.; Budach, C.; Schmidt, U. Large-scale boron-lined neutron detection systems as a ^{3}He alternative for Cosmic Ray Neutron Sensing. *Front. Water* **2020**, *2*, 16. [CrossRef]
15. Montag, B.W.; Bellinger, S.L.; Edwards, N.S.; Lage, J.; Nelson, K.A.; Henson, L.C.; McGregor, D.S. Recent progress in the commercialization of the Li Foil multi-wire proportional counter neutron detectors. *Rad. Phys. Chem.* **2019**, *155*, 158–163. [CrossRef]
16. Dimitrova-Petrova, K.; Geris, J.; Wilkenson, M.E.; Rosolem, R.; Verrot, L.; Lilly, A.; Soulsby, C. Opportunities and challenges in using catchment-scale storage estimates from cosmic ray neutron sensors for rainfall-runoff modelling. *J. Hydrol.* **2020**, *586*, 124878. [CrossRef]
17. Barker, J.B.; Franz, T.E.; Heeren, D.M.; Neale, C.M.; Luck, J.D. Soil water content monitoring for irrigation management: A geostatistical analysis. *Agric. Water Manag.* **2017**, *188*, 36–49. [CrossRef]
18. Pang, Z.; Jia, U.; Peng, X.; Ju, X.; Gau, L. Applicability of cosmic-ray neutron sensing for measuring soil water content in heterogeneous landscapes under subtropical hydroclimatic conditions. *J. Hydrol.* **2021**, *596*, 126068. [CrossRef]
19. Rasche, D.; Köhli, M.; Schrön, M.; Blume, T.; Güntner, A. Towards disentangling heterogeneous soil moisture patterns in cosmic-ray neutron sensor footprints. *Hydrol. Earth Sys. Sci. Discuss.* **2021**, 1–33. [CrossRef]
20. Soil Survey Staff; Natural Resources Conservation Service; United States Department of Agriculture. Web Soil Survey. Available online: http://websoilsurvey.sc.egov.usda.gov/ (accessed on 6 October 2021).
21. Hawdon, A.; McJannet, D.; Wallace, J. Calibration and correction procedures for cosmic-ray neutron soil moisture probes located across Australia. *Water Resour. Res.* **2014**, *50*, 5029–5043. [CrossRef]
22. Rosolem, R.; Shuttleworth, W.J.; Zreda, M.; Franz, T.E.; Zeng, X.; Kurc, S.A. The effect of atmospheric water vapor on neutron count in the cosmic-ray soil moisture observing system. *J. Hydrometeor.* **2013**, *14*, 1659–1671. [CrossRef]

23. Franz, T.E.; Wahbi, A.; Zhang, J.; Vreugdenhil, M.; Heng, L.; Dercon, G.; Strauss, P.; Brocca, L.; Wagner, W. Practical data products from cosmic-ray neutron sensing for hydrological applications. *Front. Water* **2020**, *2*. [CrossRef]
24. Desilets, D.; Zreda, M.; Ferré, T.P.A. Nature's neutron probe: Land surface hydrology at an elusive scale with cosmic rays. *Water Resour. Res.* **2010**, *46*, W11505. [CrossRef]
25. Dong, J.; Ochsner, T.E.; Zreda, M.; Cosh, M.H.; Zou, C.B. Calibration and validation of the COSMOS rover for surface soil moisture measurement. *Vadose Zone J.* **2014**, *13*, vzj2013.08.0148. [CrossRef]
26. Baatz, R.; Bogena, H.R.; Franssen, H.-J.H.; Huisman, J.A.; Montzka, C.; Vereecken, H. An empirical vegetation correction for soil water content quantification using cosmicc ray probes. *Water Resour. Res.* **2015**, *51*, 2030–2046. [CrossRef]
27. Hunter, J.D. Matplotlib: A 2D graphics environment. *Environ. Comp. Sci. Eng.* **2007**, *9*, 90–95. [CrossRef]
28. Harris, C.R.; Millman, K.J.; van der Walt, S.J.; Bommers, R.; Viranen, P.; Cournapeau, D.; Wieser, E.; Taylor, J.; Berg, S.; Smith, N.J.; et al. Array programming with NumPy. *Nature* **2020**, *585*, 357–362. [CrossRef] [PubMed]
29. McKinney, W. Data Structures for Statistical Computing in Python. In Proceedings of the 9th Python in Science Conference (SciPy 2010), Austin, TX, USA, 28 June–3 July 2010; pp. 51–56. [CrossRef]
30. Virtanen, P.; Gommers, R.; Oliphant, T.E.; Haberland, M.; Reddy, T.; Cournapeau, D.; Burovski, E.; Peterson, P.; Weckesser, W.; Bright, J.; et al. SciPy 1.0: Fundamental Algorithms for Scientific Computing in Python. *Nat. Methods* **2020**, *12*, 261–272. [CrossRef]
31. Cosh, M.H.; Jackson, T.J.; Bindlish, R.; Famiglietti, J.S.; Ryu, D. Calibration of an impedance probe for estimation of surface soil water content over large regions. *J. Hydrol.* **2005**, *311*, 49–58. [CrossRef]
32. Patrignani, A.; Ochsner, T.E.; Montag, B.; Bellinger, S. A novel lithium foil cosmic-ray neutron detector for measuring field-scale soil moisture. *Front. Water* **2021**, *3*, 673185. [CrossRef]
33. Nguyen, H.H.; Kim, H.; Choi, M. Evaluation of the soil water content using cosmic-ray neutron probe in a heterogeneous monsoon climate-dominated region. *Adv. Water Resour.* **2017**, *108*, 125–138. [CrossRef]
34. Bogena, H.R.; Huisman, J.A.; Baatz, R.; Franssen, H.J.H.; Vereecken, H. Accuracy of the cosmic-ray soil water content probe in humid forest ecosystems: The worst case scenario. *Water Resour. Res.* **2013**, *49*, 5778–5791. [CrossRef]
35. Franz, T.E.; Zreda, M.; Rosolem, R.; Ferre, T.P.A. Field validation for a cosmic-ray neutron sensor using a distributed sensor network. *Vadose Zone J.* **2012**, *11*, vzj2012.0046. [CrossRef]
36. Knoll, G.F. *Radiation Detection and Measurement*, 3rd ed.; John Wiley & Sons, Inc.: New York, NY, USA, 2000; pp. 95–103.